Occam's razor and modelling of complex phenomena in brain networks

Jaroslav Hlinka

Institute of Computer Science, Czech Academy of Sciences

MFF UK
28/02/2019

Complex Systems: neither random nor fully ordered

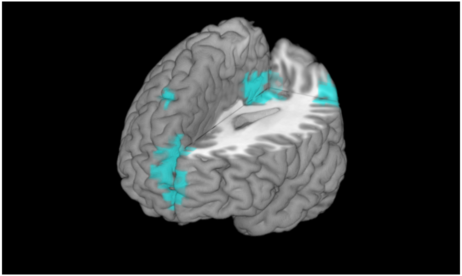

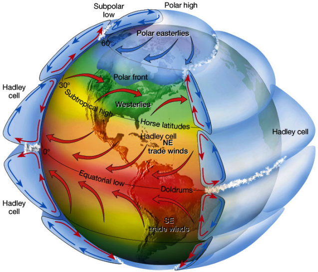

Brain: complex function, structure, dynamics

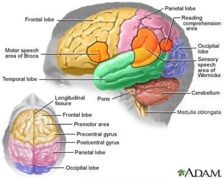

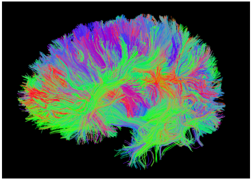

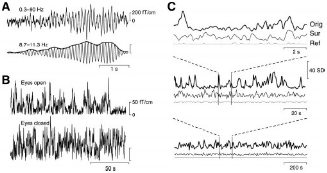

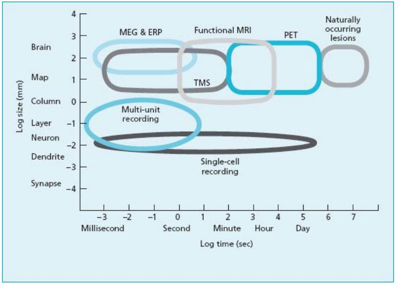

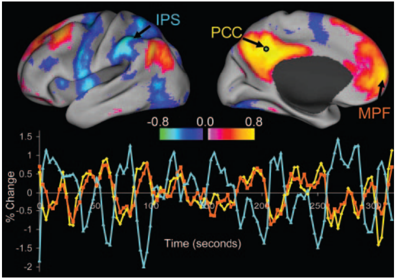

Characterizing brain state: Functional Connectivity

Characterizing brain state: Functional Connectivity

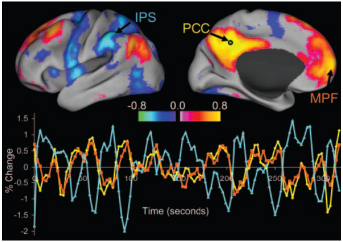

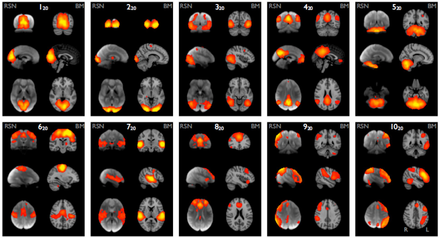

- Functional connectivity (FC): statistical dependence between activity of remote brain areas
- Typically measured by correlation of time series
- Can be measured both during resting state or a task
- In fMRI, FC is supported by LFF
- Resting networks correspond to functional brain networks

Dependence: how to measure?

Pearson's correlation $\rho_{X,Y} = \frac{\mathrm{cov}(X,Y)}{\sigma_X \sigma_Y} = \frac{E[(X-\mu_X)(Y-\mu_Y)]}{\sigma_X \sigma_Y}$

Dependence: how to measure?

Pearson's correlation $\rho_{X,Y} = \frac{\mathrm{cov}(X,Y)}{\sigma_X \sigma_Y} = \frac{E[(X-\mu_X)(Y-\mu_Y)]}{\sigma_X \sigma_Y}$
Independence(X, Y independent): $p(X, Y) = p(X)p(Y)$
Mutual information: $I(X;Y) = \sum_{y \in Y} \sum_{x \in X} p(x,y) \log\left(\frac{p(x,y)}{p(x)\,p(y)}\right)$

Dependence: how to measure?

Pearson's correlation $\rho_{X,Y} = \frac{\mathrm{cov}(X,Y)}{\sigma_X \sigma_Y} = \frac{E[(X-\mu_X)(Y-\mu_Y)]}{\sigma_X \sigma_Y}$

Independence(X, Y independent): $p(X, Y) = p(X)p(Y)$

Mutual information: $I(X; Y) = \sum_{y \in Y} \sum_{x \in X} p(x, y) \log \left(\frac{p(x,y)}{p(x)\, p(y)} \right)$

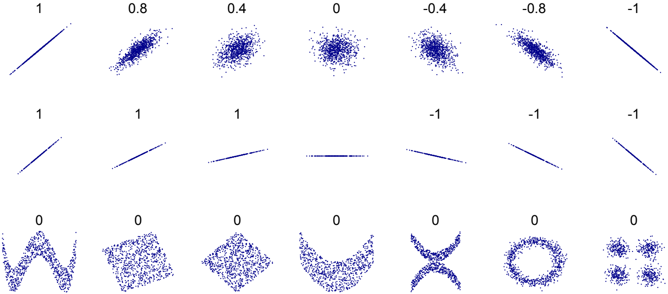

Practical problem

- linear correlation
  - widely used, simple concept
  - generally effective

Practical problem

- linear correlation
  - widely used, simple concept
  - generally effective
- BUT ... neuronal and hemodynamic processes nonlinear!

  $\Rightarrow$ nonlinear methods proposed for FC

Practical problem

- linear correlation
  - widely used, simple concept
  - generally effective
- BUT ... neuronal and hemodynamic processes nonlinear!

  $\Rightarrow$ nonlinear methods proposed for FC
- HOWEVER ... nonlinear methods also have problems!
  - robustness
  - implementation
  - interpretation

  $\Rightarrow$ **Is linear correlation sufficient for fMRI FC?**

Assumption: Gaussianity

Assumption: Gaussianity

- for bivariately normal distributions ("linear dependence"):
  - linear correlation $\rho_{X,Y}$ fully captures the dependence
  - mutual information between variables is $I(X,Y) = I_{Gauss}(\rho_{X,Y}) = -\frac{1}{2} log(1 - \rho^2_{X,Y})$
- for general bivariate distribution (under marginal normality):
  - linear correlation is not sufficient to capture the dependence
  - mutual information between variables is $I(X,Y) \geq -\frac{1}{2} log(1 - \rho^2_{X,Y})$
- $\Rightarrow$ **we can quantify the extra dependence (mutual information) that is not captured by linear correlation:** $I_{extra} = I(X,Y) - I_{Gauss}(\rho_{X,Y})$

Strategy vizualization

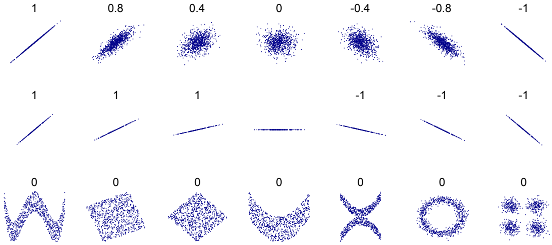

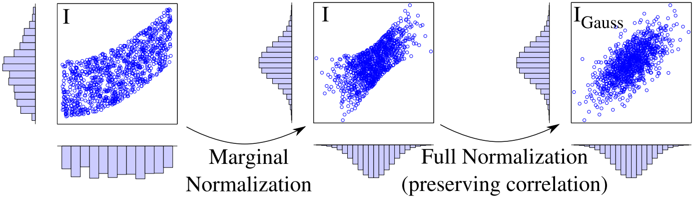

Example: brain activity dependence network (fMRI)

- **24 fMRI sessions** (3T, TR=2000 ms, $3 \times 3 \times 3.5$ mm^3, 300 volumes), standard data preprocessing
- AAL based parcellation to 90 regions
- each region represented by average activity time series
- **90-by-90 matrices of linear and nonlinear connectivity**
- **difference between linear and nonlinear connectivity**
  - **quantified**
  - **tested**
- mutual information estimated using the equiquantal method
- $I_{Gauss}(r_{X,Y})$ is estimated by computing mutual information on linearized version of the data (Fast Fourier Transform surrogates) as finite sample estimates of linear correlation and mutual information have different properties (such as bias and variance)

Results

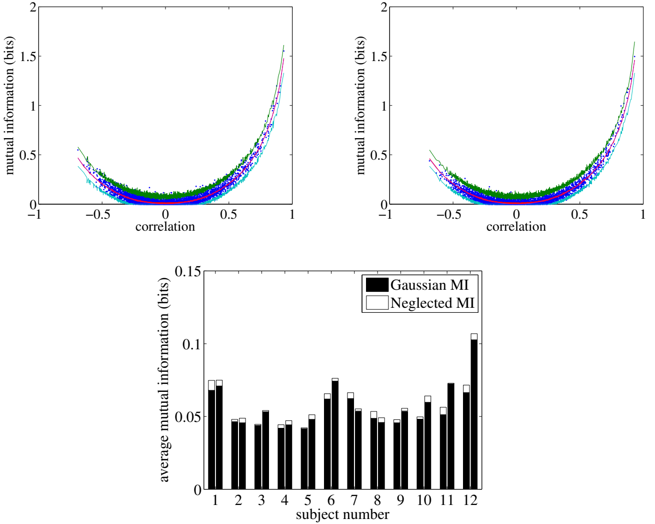

[JH et al., Neuroimage, 2011]

Nonlinear coupling in climate recordings

Nonlinear coupling in climate recordings

- Nonlinear interactions in (monthly) temperature data?

Nonlinear coupling in climate recordings

- Nonlinear interactions in (monthly) temperature data?
- nonlinear interaction:

Nonlinear coupling in climate recordings

- Nonlinear interactions in (monthly) temperature data?
- nonlinear interaction: deviation from linear interaction

Nonlinear coupling in climate recordings

- Nonlinear interactions in (monthly) temperature data?
- nonlinear interaction: deviation from linear interaction
  - existence
  - strength
  - localization
  - sources/form/origin
  - relevance for specific analysis
  - treatment

Data and methods

Data: NCEP/NCAR reanalysis dataset

- surface air temperatures
- monthly data (years 1948 - 2007; 720 timepoints)
- global grid 73 $\times$ 144 points (2.5 deg $\times$2.5 deg sampling)
- yearly cycle removed (anomalies)

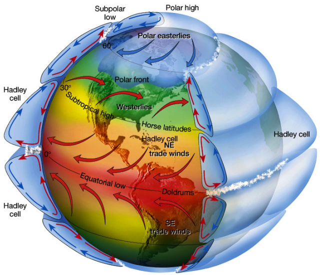

Results: Existence

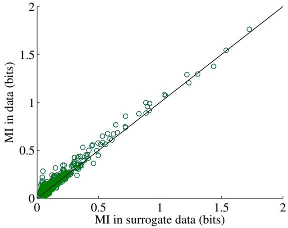

Results: Existence

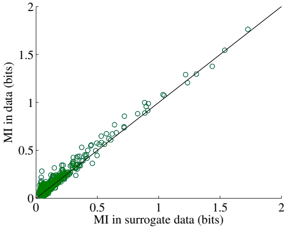

Eyeball method: not much nonlinearity
Statistical testing: 15% links above 95th percentile

Localization of nonlinear contributions

Localization of nonlinear contributions

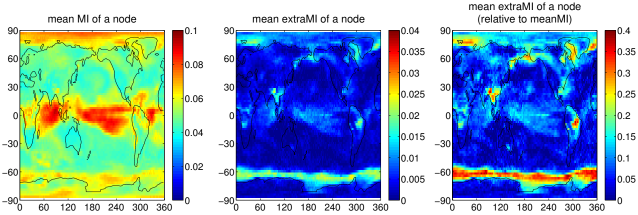

Localization of nonlinear contributions

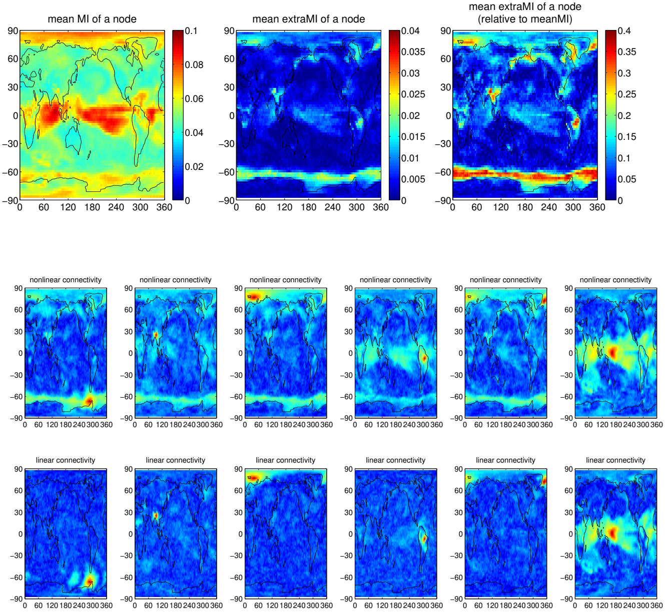

Form/origin

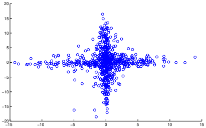

20
15
10
5
0
−5
−10
−15
−20
−15
−10
−5
0
5
10
15

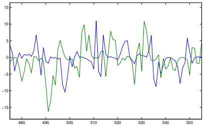

15
10
5
0
−5
−10
−15
480
490
500
510
520
530
540
550

Form/origin

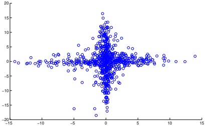

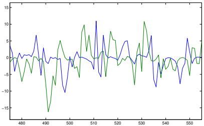

- introduce conservative preprocessing: month-wise variance equalization

Form/origin

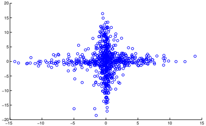

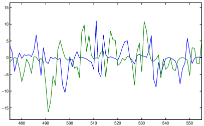

- introduce conservative preprocessing: month-wise variance equalization

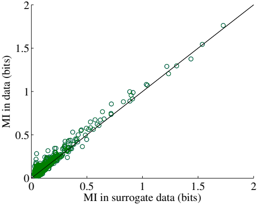

Form/origin

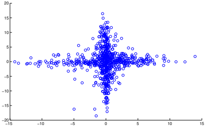

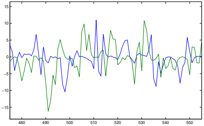

- introduce conservative preprocessing: month-wise variance equalization

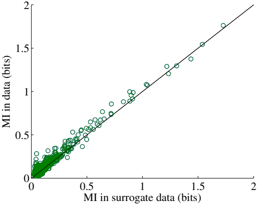

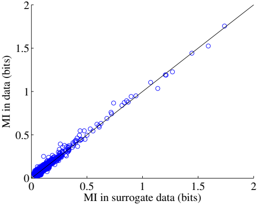

Statistical testing against surrogates: 8% links above 95th percentile

Form/origin

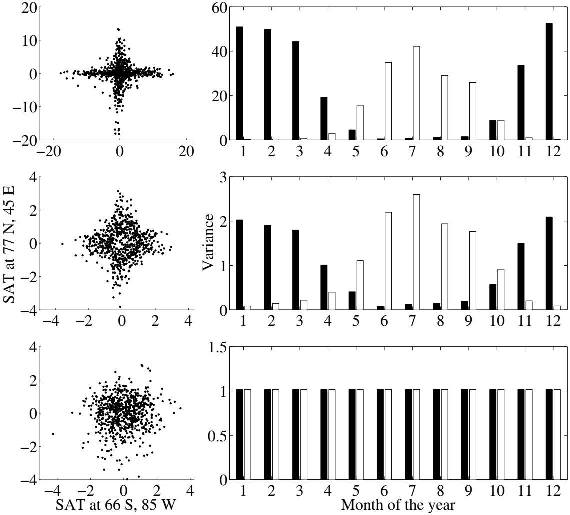

Temperature anomalies:

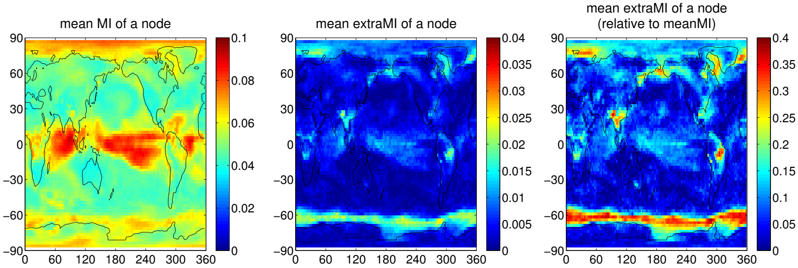

After additional normalization of variance:

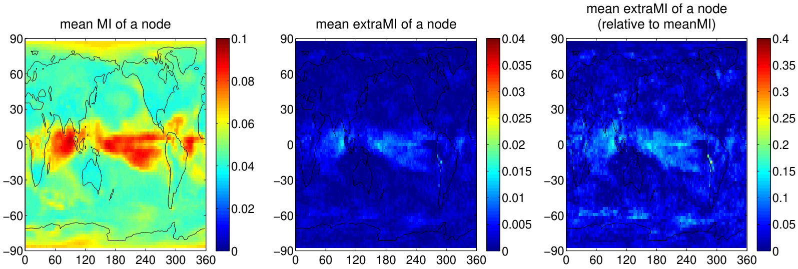

What about remaining ‘non-linearities’?

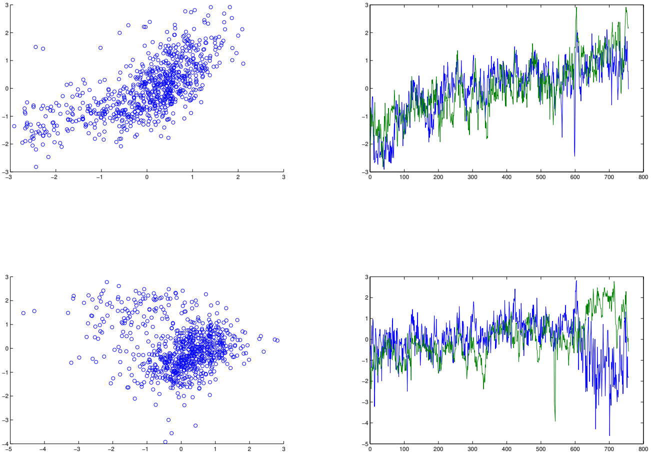

Nonstationarity ... and detecting brain states

Nonstationarity ... and detecting brain states

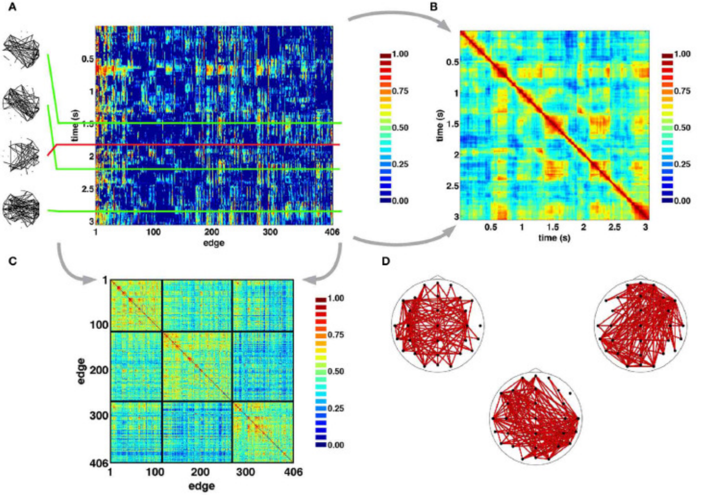

FIGURE 4 | Time series of SL networks. (A) Each row in the SL matrix corresponds to an individual network (examples are shown in the inserts at the left). These networks exhibit periods of relative topological invariance (top two inserts), abrupt transitions (third insert from the top), and recurrences (bottom insert). **(B)** Normalized cosine similarity matrix between all pairs of SL vectors for the recording period shown in **A**. Hot colors represent pairs of highly similar networks, cool colors represent dissimilarity. The presence of block structure along the diagonal of the matrix suggest periods of quasi-stability and rapid intermittent transitions. "Hot" off-diagonal patches suggest recurrences of networks. **(C)**, Cross-correlation matrix of edge time series reordered to reveal clusters of edge communities, as detected in the epoch shown in panel A. **(D)**. Plots show topographic representations of edges constituent to the communities shown at the left. As such, each edge community is the set of edges whose time courses are strongly correlated with one another.

Detecting brain states: [Betzel et al,'12],[JH et al., '15]

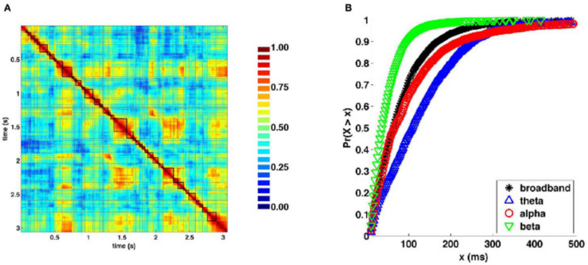

FIGURE 6 | Network states and durations. (A) Representative similarity matrix from one recording epoch (compare with **Figure 4B**) with state boundaries overlaid. **(B)** Cumulative distributions of state durations (in milliseconds) aggregated across all recording epochs and frequency bands.

Detecting brain states: [Betzel et al,’12],[JH et al., ’15]

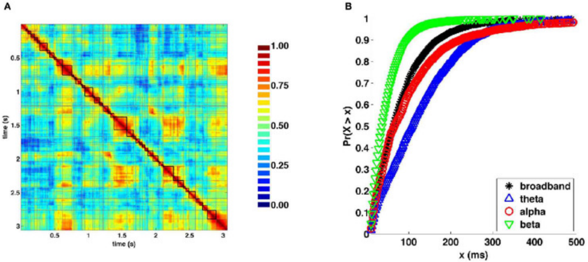

FIGURE 6 | Network states and durations. (A) Representative similarity matrix from one recording epoch (compare with **Figure 4B**) with state boundaries overlaid. **(B)** Cumulative distributions of state durations (in milliseconds) aggregated across all recording epochs and frequency bands.

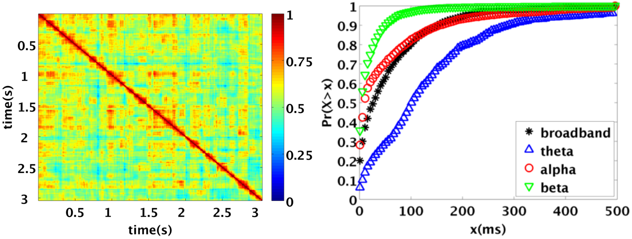

The network theory bet for real systems

The network theory bet for real systems

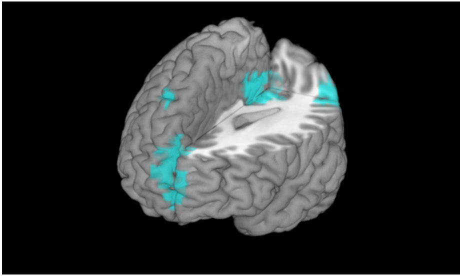

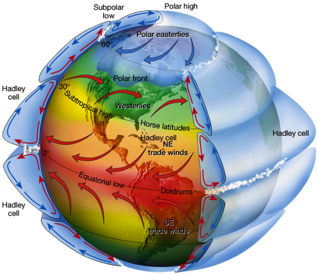

The network theory bet for real systems

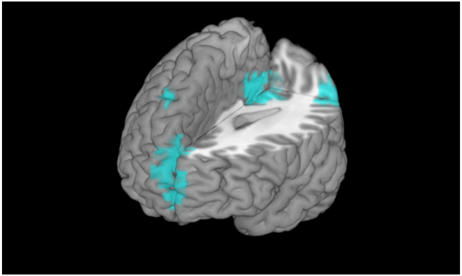

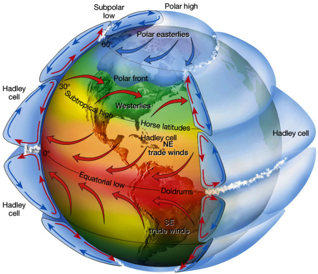

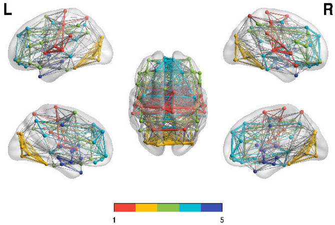

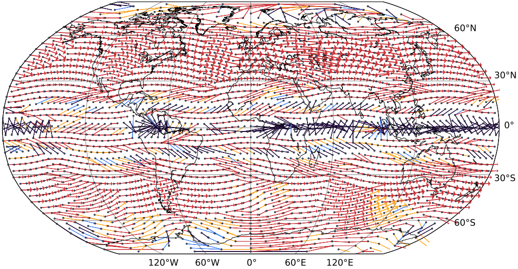

The network invasion into neuroscience

The network invasion into neuroscience

Keyword count in neuroscience (according to Scopus):

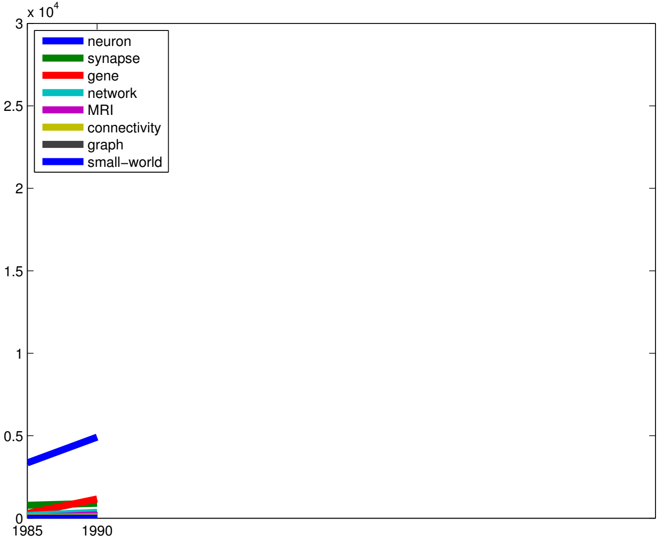

The network invasion into neuroscience

Keyword count in neuroscience (according to Scopus):

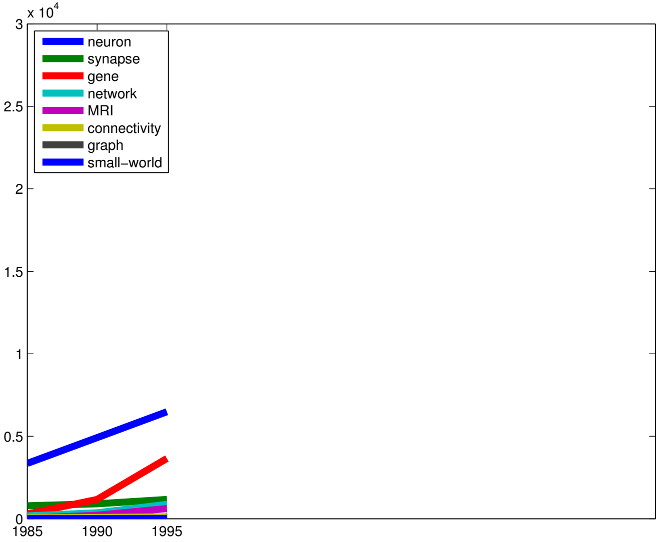

The network invasion into neuroscience

Keyword count in neuroscience (according to Scopus):

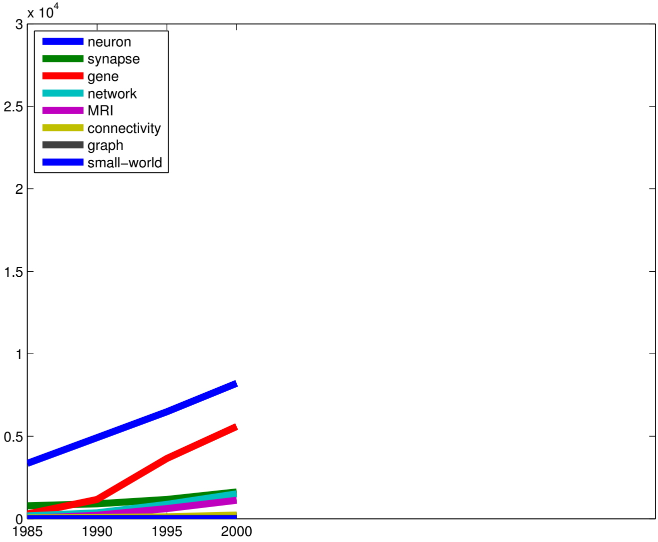

The network invasion into neuroscience

Keyword count in neuroscience (according to Scopus):

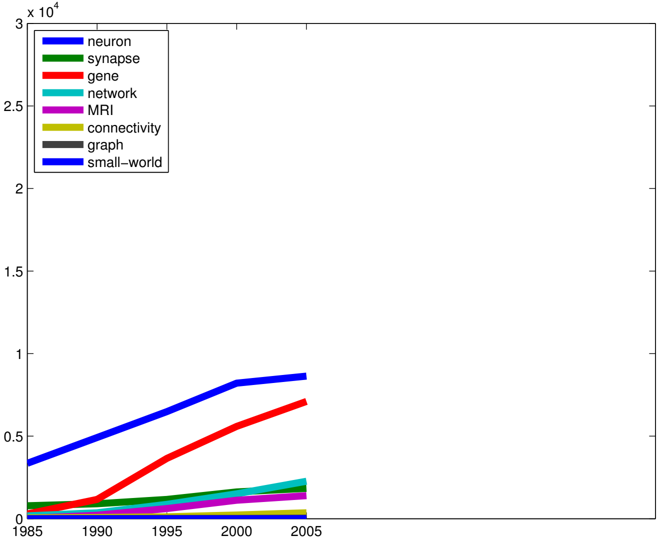

The network invasion into neuroscience

Keyword count in neuroscience (according to Scopus):

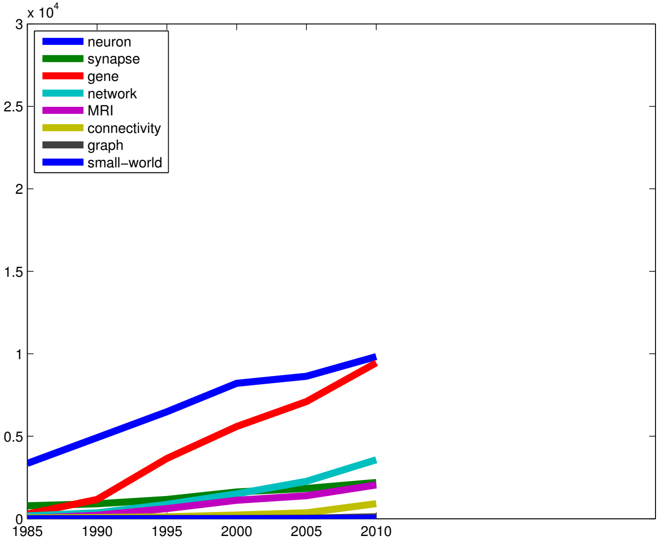

The network invasion into neuroscience

Keyword count in neuroscience (according to Scopus):

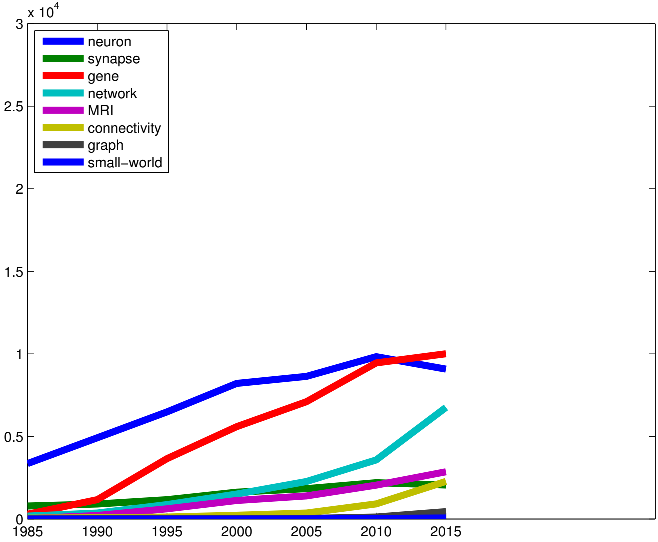

The network invasion into neuroscience

Keyword count in neuroscience (according to Scopus):

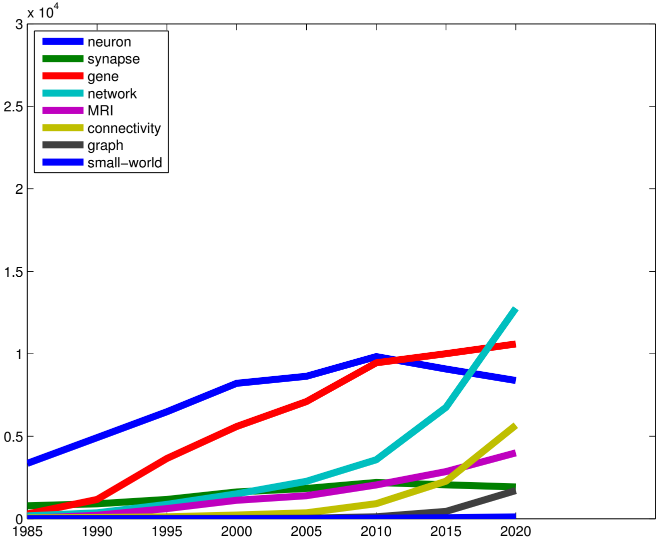

The network invasion into neuroscience

Keyword count in neuroscience (according to Scopus):

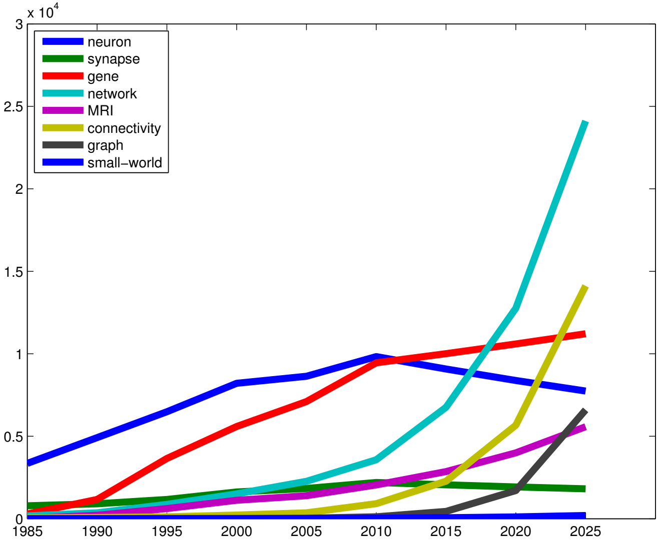

Small-world property

Small-world property

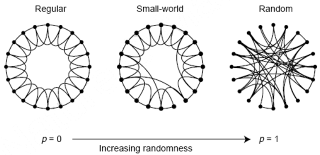

[Watts and Strogatz, 1998]

Small-world property

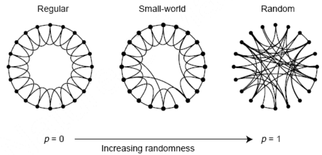

[Watts and Strogatz, 1998]

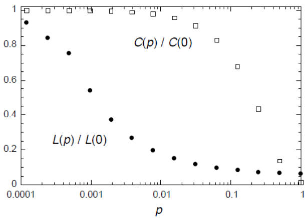

Graph: $G = (V, E)$; V set of nodes; $V = 1, \ldots, n$;$E \subset V^2$ set of edges. $d_{i,j}$ shortest path between i a j.
Reprezentation by matrix A: $A_{i,j} = 1 \Leftrightarrow (i,j) \in E$; $k_i = \sum_j A_{i,j}$ degree.

$L = \frac{1}{n \cdot (n-1)} \cdot \sum_{i,j} d_{i,j}$ $C = \frac{1}{n} \sum_{i \in V} c_i$; $c_i = \frac{\sum_{j,\ell} A_{i,j} A_{j,\ell} A_{\ell,i}}{k_j (k_j - 1)}$

small-world index ([Humphries, 2008]): $\sigma = \frac{\gamma}{\lambda} \gg 1$; $\lambda = \frac{L}{L_{rand}} \gtrsim 1$, $\gamma = \frac{C}{C_{rand}} \gg 1$

Small-world in the brain

Small-world in the brain

The brain correlation matrix is a small world:

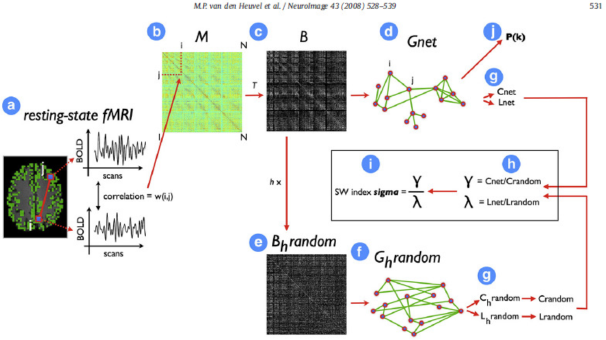

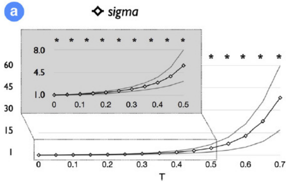

Why is this interesting?

The brain is a small world...

The brain is a small world...

and randomly connected system also...

$$X_t = AX_{t-1} + e_t$$

The brain is a small world...

and randomly connected system also...

$$X_t = AX_{t-1} + e_t$$

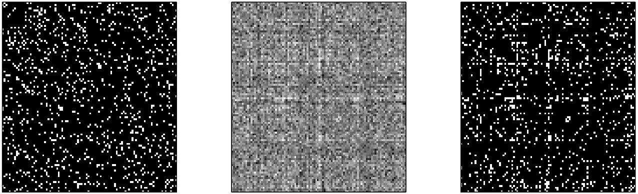

The brain is a small world...

and randomly connected system also...

$$X_t = AX_{t-1} + e_t$$

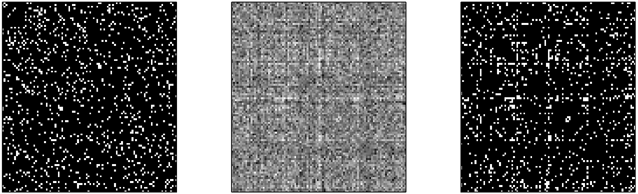

$L_S = 2.157, L_F = 2.308, C_S = 0.1081, C_F = 0.2355, \lambda = 1.07, \gamma = 2.1778, \sigma = 2.0353$. [JH et al., 2012, Chaos]

How strong is the effect?

How strong is the effect?

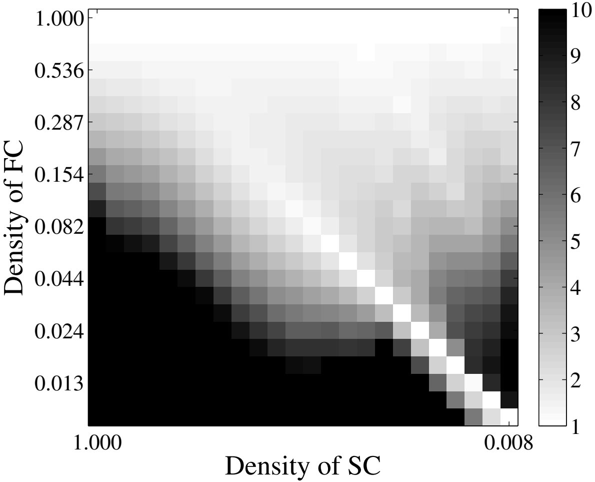

How strong is the effect?

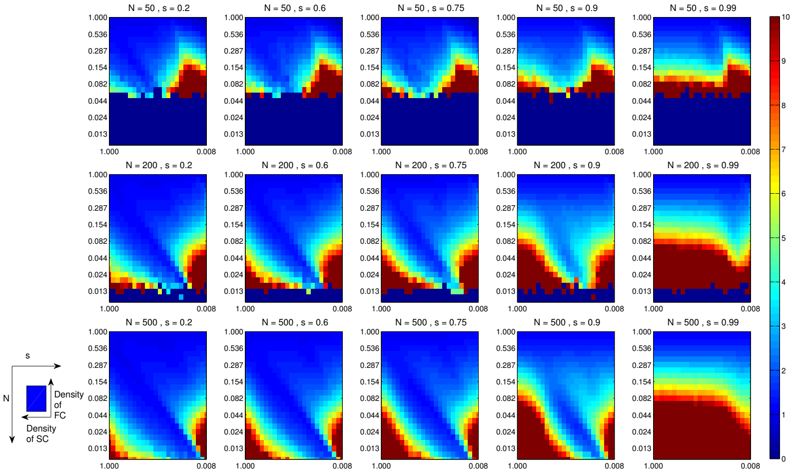

Is this the explanation for small-world in real data?

Problem: choice of the null hypotheses?

Is this the explanation for small-world in real data?

Problem: choice of the null hypotheses?
Solution: a size and coupling-distribution-matched linear vector autoregressive process

Is this the explanation for small-world in real data?

Problem: choice of the null hypotheses?
Solution: a size and coupling-distribution-matched linear vector autoregressive process

- Small-world indices were computed in the same way for data and for 'scrambled interaction' time series. This was modeled by fitting an vector autoregressive (VAR) process of order 1 to the BOLD time series:

$$X_t = c + AX_{t-1} + e_t, \tag{1}$$

  (where c is a $N \times 1$ vector of constants, A is a $N \times N$ matrix and e_t is a $N \times 1$ vector of error terms) and subsequently randomly scrambling A.
- To control for the effects of approximation by a VAR process, a realization of the fitted VAR model with scrambling omitted was also analyzed.

Data

- 10 minutes, 240 volumes of resting state fMRI (BOLD)
- 84 (48 males, mean age $\pm$ SD: 30.83 $\pm$ 8.48) healthy volunteers
- 3T Siemens Trio scanner (GE-EPI, TR/TE=2500/30 ms, voxel=3x3x3mm)
- A 3D high-resolution T1-weighted image was used for anatomical reference.
- slice-timing correction, motion correction, spatial normalization to MNI
- 90 parcels from the Automated Anatomical Labeling (AAL) atlas
- orthogonalized wrt motion parameters, white matter and CSF signal
- linear detrending, band-pass filtering (Butterworth filter 0.01 - 0.08 Hz)
- FC matrix computed by correlation and binarized to 20 percent density

Result: Brain is as ’small-world’ as if randomly rewired

Brain is as 'small-world' as ...
a size&density-matched randomly coupled linear AR(1) system.

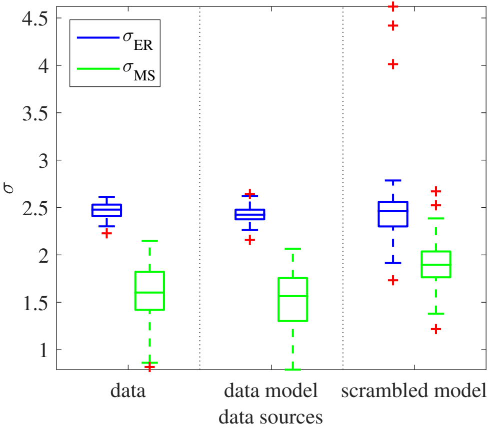

And what about the climate?

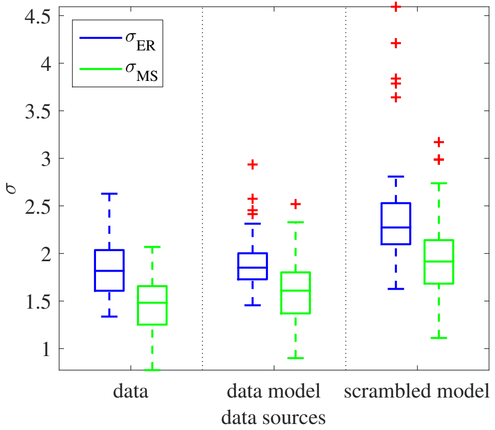

Detecting causality and measuring information flow

- Granger causality - a variable is considered causal with respect to some target variable, if its inclusion in a model improves the prediction of the target
- Bivariate Granger causality model

$$X_t^i = \sum_{\tau=1}^{+\infty} a_\tau X_{t-\tau}^i + \eta_t \qquad X_t^i = \sum_{\tau=1}^{+\infty} b_\tau X_{t-\tau}^i + \sum_{\tau=1}^{+\infty} c_\tau X_{t-\tau}^j + \phi_t$$

- Granger causality index

$$F_{X^j \to X^i} = \ln \frac{\operatorname{var}(\eta_t)}{\operatorname{var}(\phi_t)}$$

Causality - linear and nonlinear

- **Granger causality**: X 'Granger causes' Y iff including the past of Y in a (linear) model of X improves the model fit

$$F_{X^j \to X^i} = \ln \frac{\mathrm{var}(\eta_t)}{\mathrm{var}(\phi_t)} \neq 0$$

Causality - linear and nonlinear

- **Granger causality**: X 'Granger causes' Y iff including the past of Y in a (linear) model of X improves the model fit

$$F_{X^j \to X^i} = \ln \frac{\mathrm{var}(\eta_t)}{\mathrm{var}(\phi_t)} \neq 0$$

- **Transfer entropy**: the difference of entropies of Y_{t+1} conditioned on only Y_t or **also** on X_t:

$$T_{X \to Y} = I(X_t, Y_{t+1} | Y_t) = H(Y_{t+1} | Y_t) - H(Y_{t+1} | Y_t, X_t).$$

Causality - linear and nonlinear

- **Granger causality**: X 'Granger causes' Y iff including the past of Y in a (linear) model of X improves the model fit

$$F_{X^j \to X^i} = \ln \frac{\mathrm{var}(\eta_t)}{\mathrm{var}(\phi_t)} \neq 0$$

- **Transfer entropy**: the difference of entropies of Y_{t+1} conditioned on only Y_t or **also** on X_t:

$$T_{X \to Y} = I(X_t, Y_{t+1} | Y_t) = H(Y_{t+1} | Y_t) - H(Y_{t+1} | Y_t, X_t).$$

- for stationary linear Gaussian processes GC and TE **equivalent**

$$\mathcal{T}_{X \to Y} = \frac{1}{2} \mathcal{F}_{X \to Y}$$

Multivariate causal models

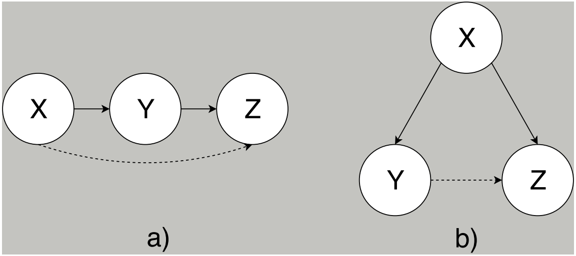

a) Indirect causality b) Spurious causality

Multivariate causal models

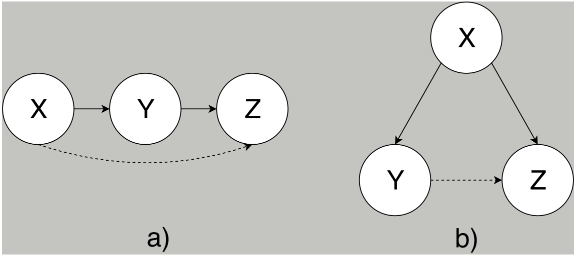

a) Indirect causality b) Spurious causality

- Multivariate Granger causality model

$$X_t^i = \sum_{\tau=1}^{+\infty} \sum_{k=1,k\neq j}^{n} d_{k,\tau} X_{t-\tau}^k + \eta_t \qquad X_t^i = \sum_{\tau=1}^{+\infty} \sum_{k=1}^{n} e_{k,\tau} X_{t-\tau}^k + \phi_t$$

- Multivariate model is necessary to distinguish between direct and indirect causality, bivariate model may also lead to detection of spurious links

Advantages of causality analysis

- provides directional information
- takes care of indirect connections (if mediating variables included)
- **but**: estimation more difficult due to higher dimensionality of variables
- proposed solutions:
  - reducing dimensionality in time and space
  - iterative estimation of conditional independence structure (Runge, PRL, 2012; Sun, Physica D, 2014; Kugiumtzis, 2012; see Hlinka et al, 2018, arxiv for comparative review)

Example: climate (temperature) interaction network

Example: climate (temperature) interaction network

Data: daily surface temperature anomalies from NCEP/NCAR reanalysis dataset on a geodesic grid
Methods: correlation vs. Granger causality

Example: climate (temperature) interaction network

Data: daily surface temperature anomalies from NCEP/NCAR reanalysis dataset on a geodesic grid
Methods: correlation vs. Granger causality

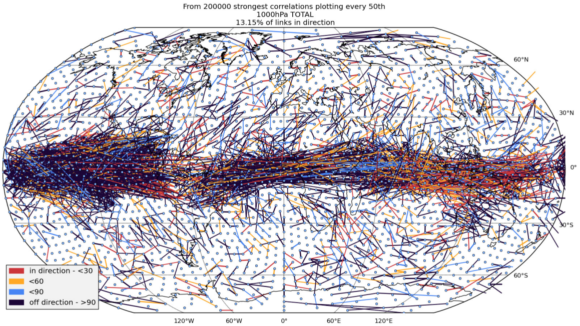

Remainder: Climate interactions (non)linearity

⇒ we can quantify the extra dependence (mutual information I) that is not captured by linear correlation ρ:

$$I_{extra}(X,Y) = I_{X,Y} - \frac{1}{2} log(1-\rho^2_{X,Y})$$

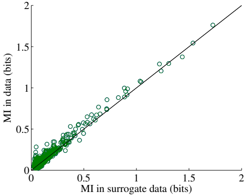

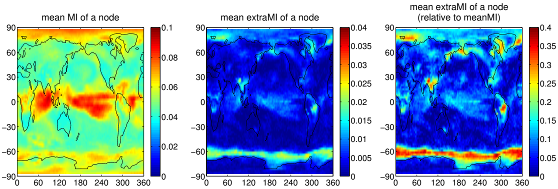

[JH et al., Climate Dynamics, 2014]

Stability of causality estimators

Nonlinear causality estimators might pay for generality with instability: linear Granger vs. estimates of transfer entropy.

Stability of causality estimators

Nonlinear causality estimators might pay for generality with instability: linear Granger vs. estimates of transfer entropy.

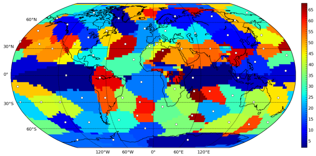

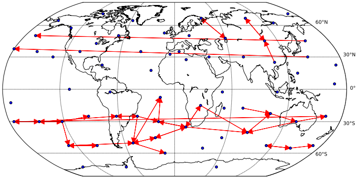

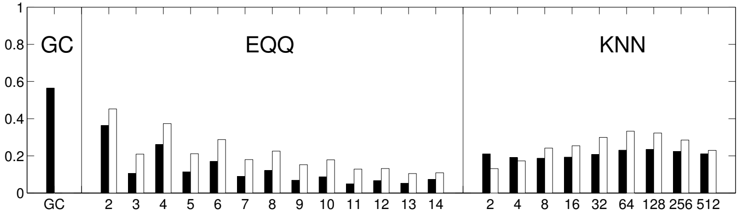

[JH et al, Entropy, 2013]

Causalities in climate

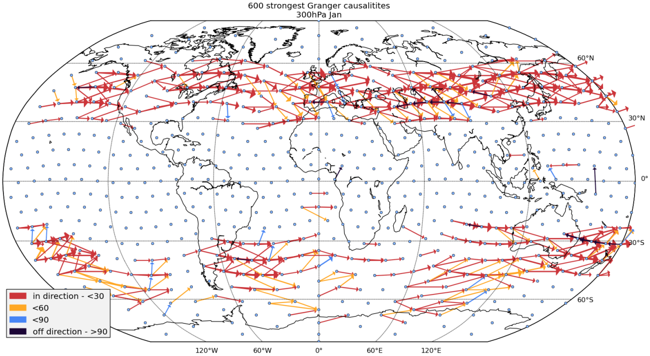

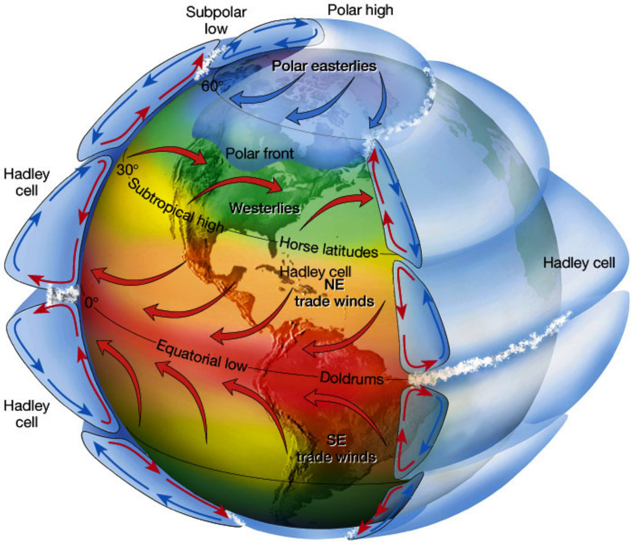
Subpolar low
Polar high
Polar easterlies
60°
Polar front
Hadley cell
30°
Subtropical high
Westerlies
Horse latitudes
Hadley cell
NE trade winds
Hadley cell
0°
Equatorial low
Doldrums
Hadley cell
SE trade winds

Winds - detail

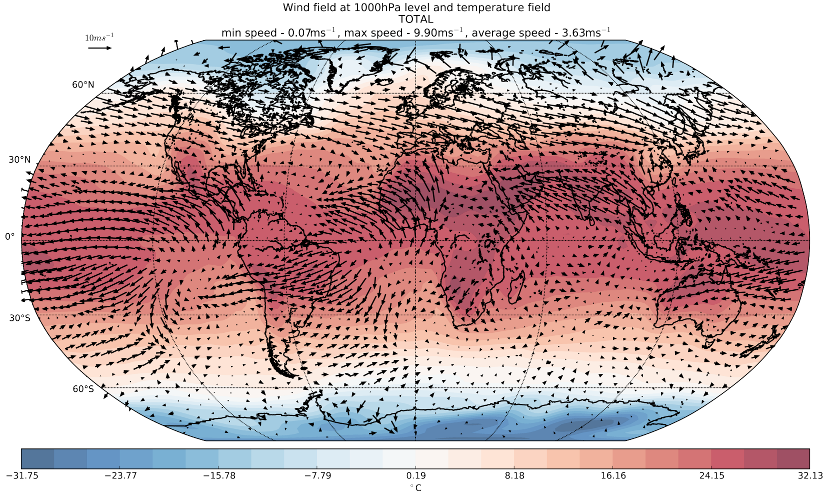

Causalities in climate - detail

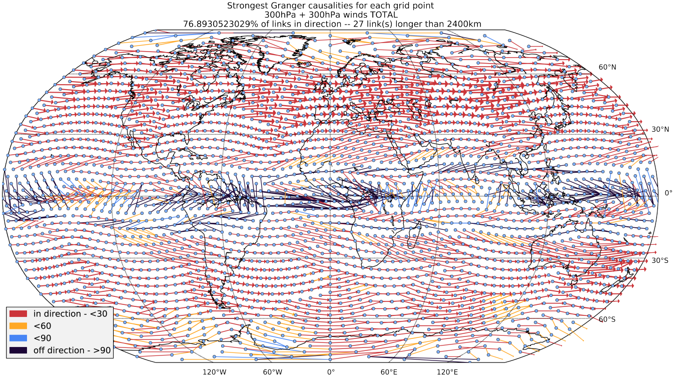

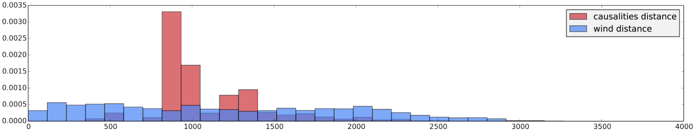

[JH et al, 2017, Chaos]

Advanced application: causal climate network

ARTICLE

Received 4 Apr 2015 | Accepted 28 Aug 2015 | Published 7 Oct 2015
DOI: 10.1038/ncomms9502
OPEN

Identifying causal gateways and mediators in complex spatio-temporal systems

Jakob Runge[1,2], Vladimir Petoukhov[1], Jonathan F. Donges[1,3], Jaroslav Hlinka[4], Nikola Jajcay[4,5], Martin Vejmelka[4], David Hartman[4,6], Norbert Marwan[1], Milan Paluš[4] & Jürgen Kurths[1,2,7,8,9]

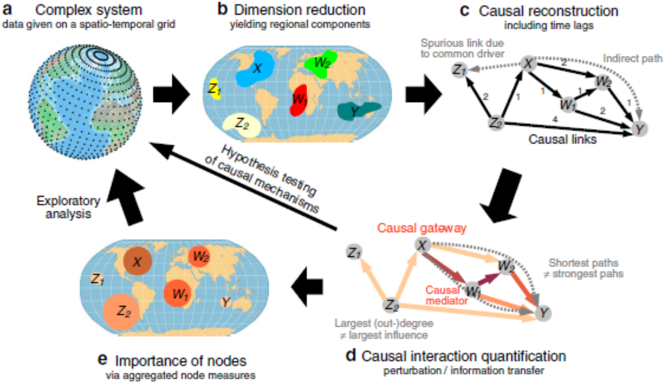

Summary

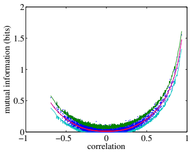

Summary

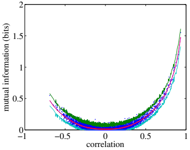

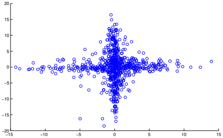

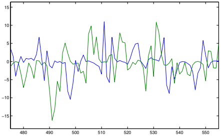

Summary

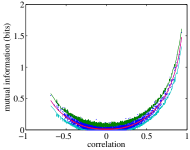

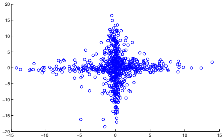

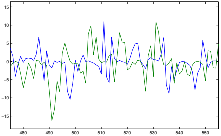

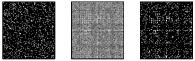

Summary

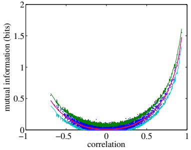

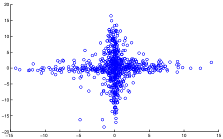

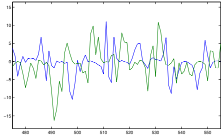

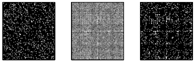

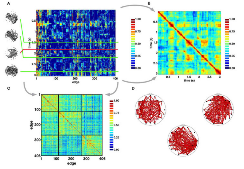

FIGURE 4 | Time series of SL networks. (A) Each row in the SL matrix corresponds to an individual network (examples are shown in the inserts at the left). These networks exhibit periods of relative topological invariance (top two inserts), abrupt transitions (third insert from the top), and recurrences (bottom insert). **(B)** Normalized cosine similarity matrix between all pairs of SL vectors for the recording period shown in **A**. Hot colors represent pairs of highly similar networks, cool colors represent dissimilarity. The presence of block structure along the diagonal of the matrix suggest periods of quasi-stability and rapid intermittent transitions. "Hot" off-diagonal patches suggest recurrences of networks. **(C).** Cross-correlation matrix of edge time series reordered to reveal clusters of edge communities, as detected in the epoch shown in panel A. **(D).** Plots show topographic representations of edges constituent to the communities shown at the left. As such, each edge community is the set of edges whose time courses are strongly correlated with one another.

Summary

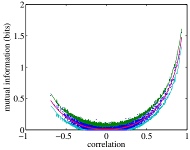

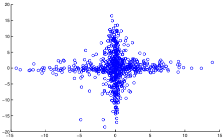

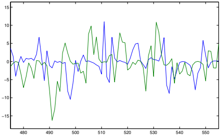

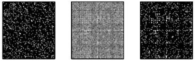

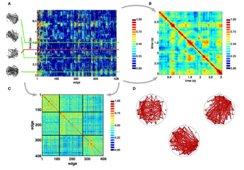

FIGURE 4 | Time series of SL networks. (A) Each row in the SL matrix corresponds to an individual network (examples are shown in the inserts at the left). These networks exhibit periods of relative topological invariance (top two inserts), abrupt transitions (third insert from the top), and recurrences (bottom insert). (B) Normalized cosine similarity matrix between all pairs of SL vectors for the recording period shown in A. Hot colors represent pairs of highly similar networks, cool colors represent dissimilarity. The presence of block structure along the diagonal of the matrix suggest periods of quasi-stability and rapid intermittent transitions. "Hot" off-diagonal patches suggest recurrences of networks. (C). Cross-correlation matrix of edge time series reordered to reveal clusters of edge communities, as detected in the epoch shown in panel A. (D). Plots show topographic representations of edges constituent to the communities shown at the left. As such, each edge community is the set of edges whose time courses are strongly correlated with one another.

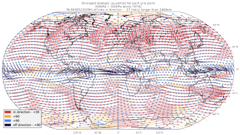

Challenges/generalizations

- large network estimation
- nonlinear interaction estimation
- event-like data
- oscillatory signals
- chaotic systems
- higher-order dependences
- nonstationarity

Thanks to my colleagues at ICS CAS, Prague, Czech Republic:
Milan Palus, David Hartman, Nikola Jajcay, Michal Hadrava,...

Thanks to my colleagues at ICS CAS, Prague, Czech Republic: **Milan Palus, David Hartman, Nikola Jajcay, Michal Hadrava,...**
and collaborators at NIMH, Klecany: **Jaroslav Tintera, Jiri Horacek, Filip Spaniel, David Tomecek,...**
and PIK, Potsdam: **Jakob Runge, Juergen Kurths, Norbert Marwan**

Thanks to my colleagues at ICS CAS, Prague, Czech Republic: **Milan Palus, David Hartman, Nikola Jajcay, Michal Hadrava,...**
and collaborators at NIMH, Klecany: **Jaroslav Tintera, Jiri Horacek, Filip Spaniel, David Tomecek,...**
and PIK, Potsdam: **Jakob Runge, Juergen Kurths, Norbert Marwan**

Open PhD and Postdoc positions at ICS CAS and NIMHCR!

Thanks to my colleagues at ICS CAS, Prague, Czech Republic: **Milan Palus, David Hartman, Nikola Jajcay, Michal Hadrava,...**
and collaborators at NIMH, Klecany: **Jaroslav Tintera, Jiri Horacek, Filip Spaniel, David Tomecek,...**
and PIK, Potsdam: **Jakob Runge, Juergen Kurths, Norbert Marwan**

Open PhD and Postdoc positions at ICS CAS and NIMHCR!
Thank you for your attention!

hlinka@cs.cas.cz

Result: Brain is as 'small-world' as if randomly rewired

Result: Brain is as ’small-world’ as if randomly rewired

Brain is as ’small-world’ as ...
a size&density-matched randomly coupled linear AR(1) system.
Different atlas (AAL, 90 regions):

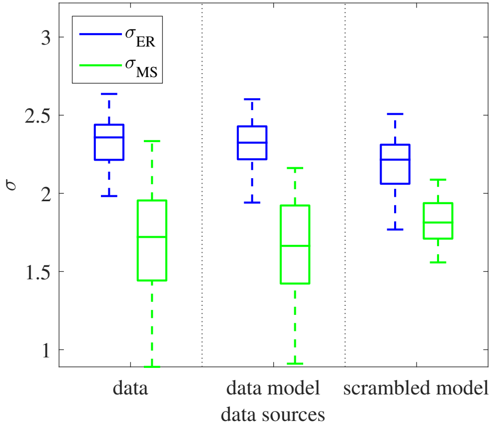

Detailed results

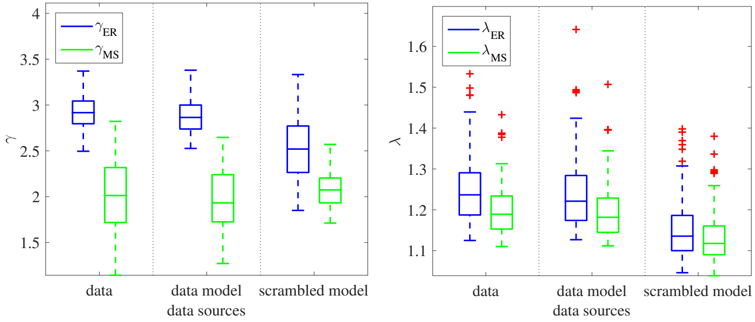

Left: relative clustering (median, quartiles, extremes, outliers) for data, VAR model and randomized VAR model.
Right: relative mean path length.

The small-world property is driven by the clustering coefficient

Modelling perturbation of epileptic dynamics

The dynamics of neural population activity is modeled by:

$$dv/dt = -\tau_x(v^3 + v^2 - a),$$

Dynamics of the population excitability parameter *a* are modelled as

$$da/dt = \tau_a(tanhc(h - v) - 0.5),$$

We set $\tau_x = 1$, $\tau_a = 0.001$, $c = 1000$ and $h = -0.44 + 1.6a$.

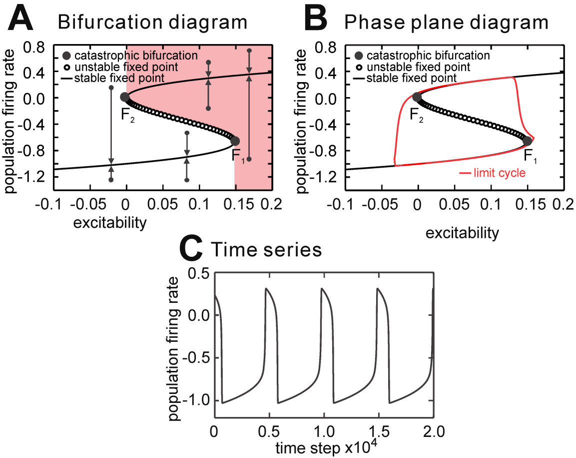
A
Bifurcation diagram
catastrophic bifurcation
unstable fixed point
stable fixed point
population firing rate
0.8
0.4
0.0
-0.4
-0.8
-1.2
F2
F1
-0.1 -0.05 0 0.05 0.1 0.15 0.2
excitability
B
Phase plane diagram
catastrophic bifurcation
unstable fixed point
stable fixed point
limit cycle
population firing rate
excitability
C
Time series
population firing rate
0.5
0.0
-0.5
-1.0
0 0.5 1.0 1.5 2.0
time step x10^4

Do perturbations cause or delays seizures?

Do perturbations cause or delays seizures?

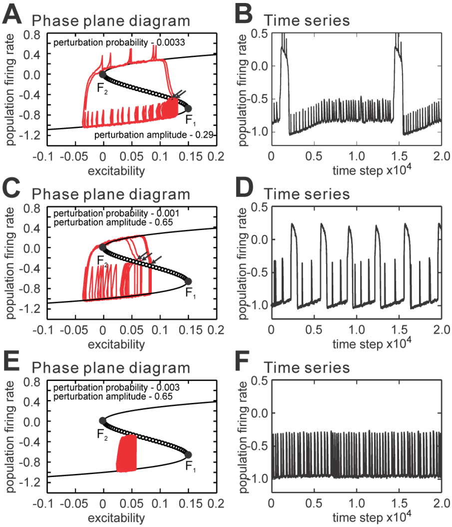

[Chang et al., submitted]

'Realistic' Epileptor model [Jirsa et al, 2014]

$$
\begin{aligned}
\frac{\mathrm{d}x_1}{\mathrm{d}t} &= y_1 - f_1(x_1, x_2, z) - z + I_{ext1} \\
\frac{\mathrm{d}y_1}{\mathrm{d}t} &= c - dx_1^2 - y1 \\
\frac{\mathrm{d}z}{\mathrm{d}t} &= r f_z(s(x_1 - x_0) + uz) \\
\frac{\mathrm{d}x_2}{\mathrm{d}t} &= -y_2 + x_2 - x_2^3 + I_{ext2} + 0.002g - 0.3(z - 3.5) \\
\frac{\mathrm{d}y_2}{\mathrm{d}t} &= \frac{1}{\tau}(-y_2 + f_2(x_2)) \\
\frac{\mathrm{d}g}{\mathrm{d}t} &= -0.01(g - 0.1x_1),
\end{aligned}
$$

$$
f_1(x_1, x_2, z) = \begin{cases} ax_1^3 - bx_1^2 & \text{if } x_1 < 0 \\ -(\text{slope} - x_2 + 0.6(z-4)^2)x_1 & \text{if } x_1 \geq 0 \end{cases}
$$

$$
f_2(x_2) = \begin{cases} 0 & \text{if } x_2 < -0.25 \\ a_2(x_2 + 0.25) & \text{if } x_2 \geq -0.25. \end{cases}
$$

Here, the x_1 and y_1 variables constitute a subsystem responsible for fast oscillations, the x_1 and y_1 variables constitute a second subsystem involved in spike wave events. The slow permittivity variable is z.

Similar dual effect in modified Epileptor

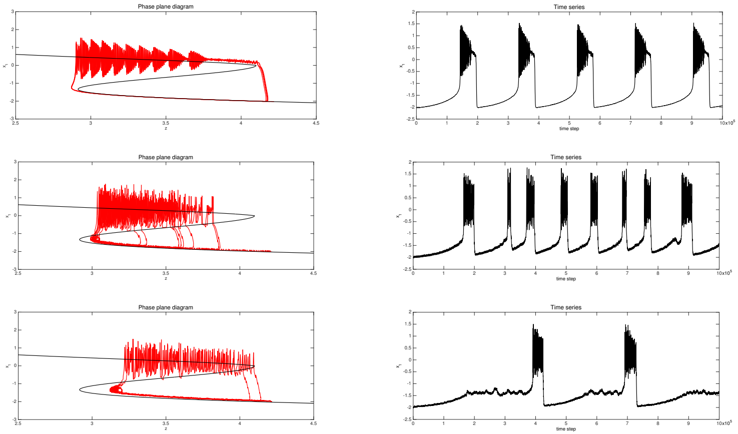

Left: phase space visualization; Right: modelled time series
Top: unperturbed model dynamics; Middle: increased seizure rate (A=1.8, P=0.0006); Bottom: decreased seizure rate (A=1.2, P=0.00018)

Why $I(X, Y) \geq -\frac{1}{2}log(1 - \rho^2_{X,Y})$?

Maximum entropy distributions:

- $(0, 1)$: uniform
- $\mathbb{R}$: does not exist, but:
- $\mathbb{R}$, $\sigma(X) = c$: $\mathcal{N}(\mu, \sigma^2)$
- $\mathbb{R}^2$, $\mathrm{Cov}(X) = \Sigma$: $\mathcal{N}(\mu, \Sigma)$

Why $I(X,Y) \geq -\frac{1}{2}log(1-\rho_{X,Y}^2)$?

Maximum entropy distributions:

- $(0,1)$: uniform
- $\mathbb{R}$: does not exist, but:
- $\mathbb{R}$, $\sigma(X) = c$: $\mathcal{N}(\mu, \sigma^2)$
- $\mathbb{R}^2$, $\mathrm{Cov}(X) = \Sigma$: $\mathcal{N}(\mu, \Sigma)$
- What about **minimal information** distribution?

Why $I(X, Y) \geq -\frac{1}{2}log(1 - \rho^2_{X,Y})$?

Maximum entropy distributions:

- $(0, 1)$: uniform
- $\mathbb{R}$: does not exist, but:
- $\mathbb{R}$, $\sigma(X) = c$: $\mathcal{N}(\mu, \sigma^2)$
- $\mathbb{R}^2$, $\text{Cov}(X) = \Sigma$: $\mathcal{N}(\mu, \Sigma)$
- What about **minimal information** distribution?
  - $I(X; Y) = H(X) + H(Y) - H(X, Y)$
  - $\arg\min_X I(X) \stackrel{?}{=} \mathcal{N}(\mu, \Sigma)$

Why $I(X, Y) \geq -\frac{1}{2}log(1 - \rho^2_{X,Y})$?

Maximum entropy distributions:

- $(0, 1)$: uniform
- $\mathbb{R}$: does not exist, but:
- $\mathbb{R}$, $\sigma(X) = c$: $\mathcal{N}(\mu, \sigma^2)$
- $\mathbb{R}^2$, $\mathrm{Cov}(X) = \Sigma$: $\mathcal{N}(\mu, \Sigma)$
- What about **minimal information** distribution?
  - $I(X; Y) = H(X) + H(Y) - H(X, Y)$
  - $\arg\min_X I(X) \stackrel{?}{=} \mathcal{N}(\mu, \Sigma)$
  - Yes, if we fix $H(X)$ and $H(Y)$ by marginal normalization...

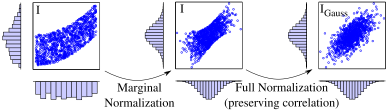

  - **Is this needed?**